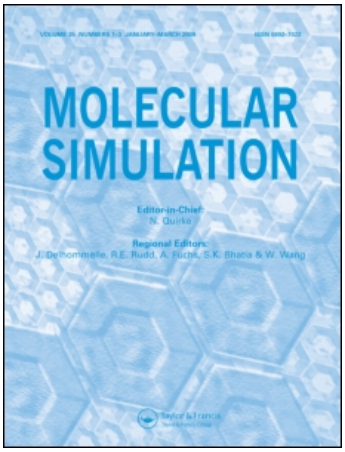

Molecular Simulation
Publication details, including instructions for authors and subscription information:
http://www.informaworld.com/smpp/title~content=t713644482

The Effect of a Crystalline Environment on Calculated Electron Densities

Robin W. Grimes[ab]
[a] Department of Chemistry, University of Keele, Keele, Staffs., UK [b] The Royal Institution of Great Britain, London

To cite this Article Grimes, Robin W.(1990) 'The Effect of a Crystalline Environment on Calculated Electron Densities', Molecular Simulation, 5: 1, 9 — 22
To link to this Article: DOI: 10.1080/08927029008022408
URL: http://dx.doi.org/10.1080/08927029008022408

Molecular Simulation, 1990, Vol. 5, pp. 9–22
Reprints available directly from the publisher
Photocopying permitted by license only

THE EFFECT OF A CRYSTALLINE ENVIRONMENT ON CALCULATED ELECTRON DENSITIES

ROBIN W. GRIMES*

Department of Chemistry, University of Keele, Keele, Staffs., ST5 5BG, UK

(*Received November 1989, accepted November 1989*)

Central to the calculation of useful interatomic potentials is a reliable determination of the electron densities of interacting ions. When the ions are embedded in a crystalline environment, it is reasonable to expect the effect of the crystal to be important in such calculations.

For certain ions (for example Mg^{2+} ions in MgO) the crystal has little effect on ion electron densities. Conversely, ions such as O^{2-} can only exist as a result of the stabilizing influence of lattice potentials; consequently, they are significantly modified by different lattice environments.

This paper will discuss the relevance of lattice effects to ions in MgO, in particular, Mg^{2+}, Mg^{+}, O^{2-} and F^{-}. Of these examples, the defect ions Mg^{+} and F^{-} are used to demonstrate how, in certain circumstances, the usual assumption that cations are not affected by lattice potentials but that anions are greatly influenced is not applicable. This work also emphasises the role of embedding electron-electron interactions in addition to the Madelung potential.

KEY WORDS: Interatomic potentials, electron densities, environmental effects.

1. INTRODUCTION

In early Born lattice models, short range interatomic potentials were chosen using empirical fitting procedures [1]. Generally, this consisted of determining the parameters of a convenient functional form so that calculated lattice properties were in agreement with experimental data. Since then, however, it has been realised that perfect lattice fitting procedures cannot always provide parameters useful for calculating defect properties [2, 3]. This is because potentials determined from bulk lattice properties may only be appropriate to model small interatomic displacements around equilibrium lattice sites. In problems that relate to charged defects, ion relaxations can be quite considerable (this point is dicussed in the paper by Harding [3]). Also, in many cases the available experimental data is not sufficient to provide for the fitting process. The alternative to fitting procedures is to calculate short range potentials directly.

Two computational procedures have become important for calculating short range pair interactions. The first method is based on a density functional treatment of a uniform electron gas [4–7]. In this, interaction terms which represent kinetic, exchange, coloumb and correlation energies are expressed as functions of the electron densities of interacting ions (this is discussed further in the paper by Alan [7]). Electron densities are usually obtained from single ion Hartree-Fock self-consistent-field molecular orbital calculations, although it is sometimes necessary to solve the relativistically correct Dirac-Fock equations instead (see the article by Pyper [8]). In

*Present address: The Royal Institution of Great Britain, 21 Albemarle St., London W1X 4BS.

the second method, potentials are extracted directly from Hartree-Fock cluster calculations by considering changes in total energy caused by distortions to the cluster geometry [9–11]. Parameters of a functional form are chosen so that distortions of a classical Born model cluster have the same total energy dependence as the quantum cluster. It is important to note that cluster calculations will implicitly account for modifications to the ion wavefunctions caused by distortions to the lattice site while electron gas methods generally assume a rigid electron density.

Central to both potential generating methods is a reliable determination of the wave functions (and hence electron densities) of interacting ions. Since in solid state problems we are concerned with ions embedded in a lattice, the effect of the embedding potential on ion wave functions must therefore be of concern. The purpose of this paper is to discuss the ways in which lattice potentials may affect both host (lattice) and impurity ion wave functions. Throughout the discussion, each point will be illustrated by an example involving an ion embedded in the MgO lattice.

The effect of lattice environments on calculated ion properties has been the focus of a number of previous studies. In work on LiF [12], BeO and MgO [13] by Broughton and Bagus and in studies on alkali halides [14] and MgO [15] by Fowler and Madden, the influence of an embedding lattice was investigated through a partition of lattice effects into two terms (initially considered by Mahan [16]). The first term was the Madelung potential, a consequence of having a lattice of positive and negative point ions. The second term was due to electron-electron interactions, thereby attributing a finite size to nearest neighbour ions. The results of these previous studies show that in MgO both terms act to contain (and compress) the electron density of the O^{2-} ion, but that neither term has much effect on the size of the Mg^{2+} ion. Results of the present work support these conclusions for lattice Mg^{2+} and O^{2-} ions.

Lattice effects are considered to be important in calculating reliable ion polarisabilities [14–17]. A comprehensive review of this is given in a preceding article [17]. Through this work, it has been noted [14] that lattice potentials change anion electron densities much more than they affect cation densities. Indeed, it was in an attempt to calculate the polarisability of the O^{2-} ion that Watson [18] showed that an applied Madelung field was able to stabilize the second negative charge around the O^{-} ion centre. Without this lattice potential the O^{2-} ion is not stable. It should be noted that in the present calculations, a point ion array is used to generate a Madelung potential and not a Watson sphere since it has been found that the latter tends to underestimate the compressional effect of an applied Madelung potential [15].

2. CALCULATIONS

All calculations involve the solution of Schrödinger's equations *ab initio* to Hartree-Fock level in a self-consistent-field manner. Initially, in order to provide a reference point, a single isolated ion calculation is performed. Following this, the ion is embedded in a point ion array that simulates the effect of a crystalline Madelung field. The array consists of 86 point charges positioned at perfect lattice sites in consecutive shells surrounding the quantum mechanically modelled ion. Thus, we are modelling lattice ions as fixed point charges; the ion positions are not altered during the calculation. The charge of a point ion in the five inner shells is equal to the formal charge appropriate to the corresponding lattice site. The ions in the two outermost

shells have non-integral charges, these values being chosen to give the Madelung potential and electrostatic fields at the central and nearest neighbour sites that would be expected from an infinite point ion array. Details of the point charge array have been given in a previous publication [19].

It is important that correct Madelung potentials and electrostatic fields are generated at nearest neighbour sites, since the next step in these calculations is to replace the nearest neighbour point charges by ions that are modelled in the quantum cluster (see Figure 1). Thus, the effects of electron-electron interactions from nearest neighbour ions are included in the lattice model. These interactions are electron repulsion and exchange, and they act to compress the electron density of the central ion through an effective Pauli or orthogonalization potential.

Some of the calculations that we shall be concerned with involve charged defects whose nearest neighbour O^{2-} ions are modelled in the quantum cluster. For these cation substitutional defects' the oxygen ions will polarize in response to the defect (this has been considered in detail in a recent article [19]). To model polarizable ions correctly, it is necessary to use a quantum cluster that incorporates unpolarizable Mg^{2+} ions in (200) positions (see Figure 1, section 3.2.2 and 3.3.1).

Polarization is an attempt by the lattice to redress the imbalance in electrostatic forces caused by the defect. As a consequence of polarization, the lattice potentials that acted on the central ion's electron density are changed. This is a manifestation of the third effect that we shall discuss: changes to electron densities due to lattice relaxation. It is, of course, only of relevance to a defective lattice.

2.1 Basis sets

In addition to compression and polarization, including nearest neighbour ions in the quantum cluster increases the number of basis functions available to the molecular orbital calculation. This can lead to a phenomenon known as basis set superposition error [19]. The best way of avoiding this is to use good quality flexible basis sets for all ions in the quantum cluster.

In this study, triple-zeta Gaussian GAMESS library basis sets [20] are used to represent anions. For the O^{2-} ion, this is a 62111-311 type basis; that is, it employs five independent *s*-type and four independent *p*-type orbitals. In a recent study [19], such a high quality basis was found to be necessary for the calculation of reliable defect formation energies. Since most cations are relatively less diffuse than anions, it is usually possible to use a less computationally expensive atomic basis set for cations, while maintaining the same level of success in defect calculations. For this study we use split valence 3-21G GAMESS library basis sets for cations. All calculations were carried out using the GAMESS code [20].

3. RESULTS AND DISCUSSION

The results of this study are discussed with reference to changes in Mulliken gross atomic populations [21] and in one-electron eigenvalues (energy levels). Although Mulliken populations are not always considered the most suitable way to investigate ion size defects, in the present context, since we compare populations from like-ions, they will provide a clear indication of how electron density is altered by the implementation of different lattice models. When considering molecular clusters (Figure 1),

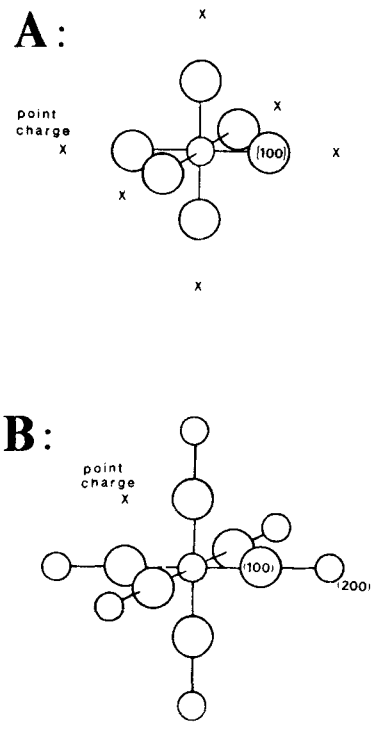

Figure 1 Clusters used to investigate the effect of nearest neighbour electron densities on the central ion wavefunction. A: the small cluster is used when the centre is an anion and the (100) ions are cations. B: the larger cluster is used when the centre and (200) ions are cations and the (100) ions are anions.

even with the high quality basis sets used in this study, it was found that basis set superposition caused a small unphysical overpopulation of valence functions. In these cases, the valence function populations were modified by considering a virtual-only basis set superposition calculation [19].

In Tables I–VI, the basis functions are ordered so that *s*-type functions preceed *p*-type. The functions also have a numerical ordering that reflects their spatial extent. For example, in Table I, for Mg^{2+} *s*-type basis functions, the "*s*1" function is the least diffuse and the "*s*4" function is the most diffuse. By considering this ordering, if a change in ion environment causes the population of an *s*3 basis function to increase at the cost of an *s*4 function, the electron density of *s*-orbitals can be said to have contracted.

It is important to make a clear distinction between basis functions designated as *s*1, *s*2, *p*1, *p*2 etc. and the molecular orbitals, 1*s*, 2*s*, 2*p* etc. since the latter are, of course, linear combinations of the former.

3.1 The effect of a point ion array

3.1.1 The lattice ion Mg^{2+}

Figure 2 shows the energy level values for an isolated gas phase Mg^{2+} ion. In the 2+

Table 1 Mulliken gross atomic basis function populations for Mg^{2+}

Atomic basis functions	*Gas phase Mg^{2+} ion*	*Mg^{2+} ion in point charge array*	*Population of Mg orbitals in embedded $[MgO_6Mg_6]^{2+}$*
*s*1	1.9989	1.9989	1.9984
*s*2	0.9772	1.9774	1.9864
*s*3	0.0378	0.0388	0.0519
*s*4	−0.0139	−0.0151	−0.0367
*p*1	1.9635	1.9626	0.9513
*p*2	0.0412	0.0426	0.0439
*p*3	−0.0047	−0.0051	−0.0048

charge state, magnesium is a stable gas phase ion and the energy levels are doubly occupied up to, and including, all 2*p* levels. The Mg^{2+} ion is therefore a closed shell **S** state ion (as indeed is the O^{2-} lattice ion).

If the ion is now surrounded by the point ion array, all the energy levels are raised in value by 23.89 eV. This positive shift in energy is exactly the repulsive interaction expected from the Madelung potential for an electron bound to a magnesium site in MgO (see Figure 3). For the Mg^{2+} ion, the Madelung potential will be attractive since the ion is positively charged.

The point charge array was chosen to mimic, at the central magnesium site, the Madelung potential and electrostatic fields generated by an infinite point ion array. This observed change in energy level values is consistent with the premise that the Mg^{2+} wavefunction is *unaltered* by the point charge array. This is confirmed by the Mulliken populations reported in Table I. These show that the gas phase ion populations and the populations of the ion in the point charge array are practically identical,

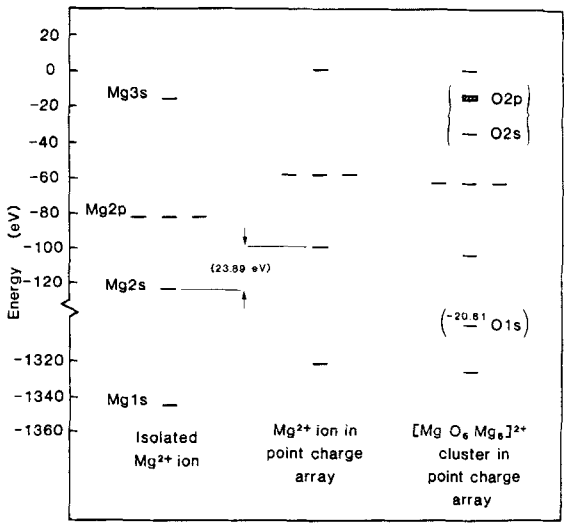

Figure 2 Mg^{2+} ion energy levels calculated for the gas phase ion and for the ion embedded in two different lattice-model environments.

and hence the electron densities are effectively the same. This can be expressed algebraically. For a gas phase ion,

$$\mathbf{H}_g\psi = \mathbf{E}_g\psi \quad (1)$$

where $\mathbf{H}_g$ is the usual atomic Hamiltonian for Schrödinger's equation, $\mathbf{E}_g$ are the eigenvalues, and ψ is the ground state wave function. Consistent with the calculated results, we may propose a model in which the Madelung potential is included into equation 1 to give,

$$(\mathbf{H}_g + \mathbf{V}_m)\psi = (\mathbf{E}_g + \mathbf{E}_m)\psi \quad (2)$$

where $\mathbf{V}_m$ is the Madelung operator (as generated by the point ion array). In this model $\mathbf{V}_m$ acts only to add a constant, $\mathbf{E}_m$ (the Madelung potential energy), to the eigenvalues; the wave function remains unaltered. Since equation (2) is separable, the model suggests that the Madelung potential is flat over the spatial extent of the Mg^{2+} ion's ground state wave function.

Figure 3 depicts the spherically averaged Madelung potential calculated for the point charge array (as described by Mahan [16]). It is at once evident that the Madelung well is indeed flat out to nearest neighbour centres (2.106 Å). This is a much greater distance than the Mg^{2+} ion radius (0.72 Å) [22].

3.1.2 The lattice ion O^{2-}

Figure 4 shows that energy levels calculated for the O^{2-} ion embedded in the appropriate point charge array are lower in energy than those calculated for the gas phase ion. This reduction in eigenvalue occurs because the Madelung potential at the oxygen site is attractive to electrons (see Figure 5). However, not all energy levels are reduced in energy to the same extent, and, none are reduced by as much as the Madelung energy (23.89 eV). (The average reduction is 23.27 eV.)

By considering the Mulliken populations calculated for the gas phase and point charge embedded O^{2-} ion wave functions (Table II), we can see that the effect of the point charge array is to induce a charge redistribution. In particular, the $p3$ basis function which has a population of 0.824 electrons for the gas phase wave function has a population of only 0.798 when the O^{2-} ion is embedded in the point charge array. Conversely, the population of the less diffuse $p2$ atomic function increases to

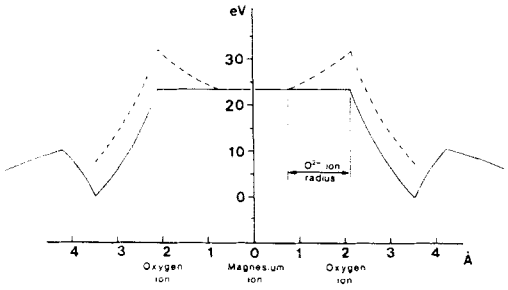

Figure 3 Simulated lattice potentials experienced by electrons bound to the Mg^{2+} site. The solid line represents the Madelung potential generated by the point ion array. The dashed lined includes the effect of nearest neighbour O^{2-} ion electron density.

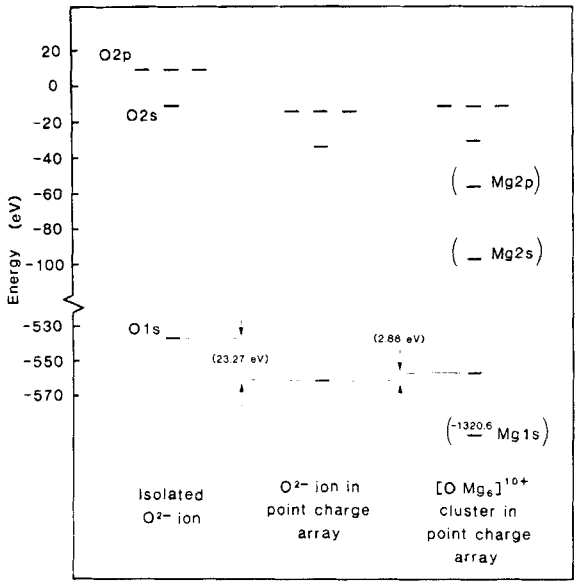

Figure 4 O^{2-} ion energy levels calculated for the gas phase ion and for the ion embedded in two different lattice-model environments.

0.539 for the embedded O^{2-} ion from a gas phase value of 0.514 electrons. Since the oxygen *p*2 basis function is less diffuse than the *p*3, the overall O^{2-} *p*-type electron density is shown to have been contracted by the point ion array. Although the results in Table II indicate that the point charge array has caused the oxygen *s*-type functions to slightly extend their charge density, the contraction in the *p*-type charge density is three times greater. Also, since there are three times more *p* electrons than there are *s* electrons, it is clear that the overall effect of the embedding point ion array has been to contract the O^{2-} electron density; that is, to confine it to a smaller atomic volume.

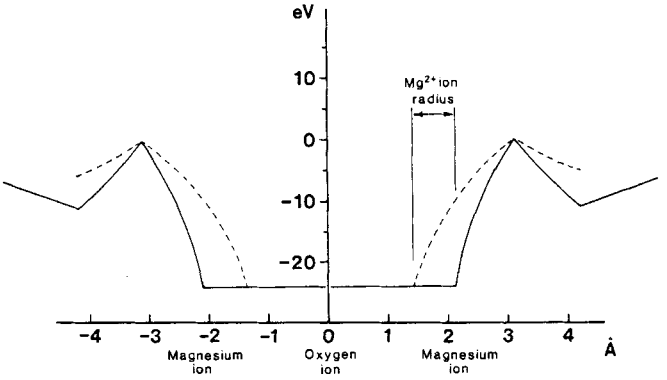

Figure 5 Simulated lattice potentials experienced by electrons bound to the O^{2-} site. The solid line represents the Madelung potential generated by the point ion array. The dashed line includes the effect of nearest neighbour Mg^{2+} ion electron density.

Table 2 Mulliken gross atomic basis function populations for O^{2-}

Atomic basis functions	*Gas phase O^{2-} ion*	*O^{2-} ion in point charge array*	*Population of O^{2-} orbitals in embedded $[OMg_6]^{m+}$ cluster*
*s*1	1.0649	1.0647	1.0637
*s*2	0.8673	0.8675	0.8689
*s*3	0.1909	0.1901	0.1713
*s*4	0.8604	0.8514	0.8603
*s*5	0.0166	1.0262	0.9972
*p*1	0.6614	0.6632	0.6851
*p*2	0.5143	0.5391	0.6486
*p*3	0.8243	0.7977	0.6791

This observation is consistent with the results of other studies [13, 15].

To understand why the O^{2-} ion charge density is confined by the point charge array, it is necessary to consider the shape of the electrostatic potential created by the point ion array. This is shown in Figure 5. The potential is essentially "well" shaped so that any diffuse electron density extending beyond the flat bottom of the well is subjected to a restraining force due to the potential well sides. Since the calculated gas phase O^{2-} ion electron density is very diffuse, it will interact with the potential well sides.

Forcing the electrons to occupy a smaller atomic volume, increases the ion's electron density. This leads to an increase in the ion's kinetic energy, as the relationship between kinetic energy (k.e.) and electron density (ρ) is approximately k.e. $\alpha\ \rho^{5/3}$ [7]). Electron–electron repulsive terms also increase. If considered alone, these increases in energy, will cause the one-electron eigenvalues to become less negative. However, we also have a dominant Madelung term which reduces the eigenvalues through the potential term ($\mathbf{V}_m$) described in equation (2). Consequently, we may state that the decrease in eigenvalue is not as large as $\mathbf{V}_m$ because of the compressive force of the well sides.

The results that have been presented in this section concern the gas phase O^{2-} ion. Implicit in this is the assumption that an O^{2-} ion can be described by a localised electron density description. In fact, experimentally, the O^{2-} anion is not a stable gas phase species, the second negative charge is not bound to the O^- centre. If we had used a basis set that included more diffuse functions, the resulting O^{2-} wave function would have incorporated linear components of the diffuse functions in the 2*p* molecular orbital description. Essentially, with a $2p^6$ orbital occupation, the oxygen ion will have significant electron density extending as far as the basis set flexibility will allow. However, because of the Madelung potential, the O^{2-} ion is stable in many ionic crystals. In such cases, the basis functions need only include components that model electron densities that are as diffuse as the extent of the bottom of the Madelung well.

3.1.3 The F^- defect ion

Although F^- is an anion, it is evident from the Mulliken populations of Table III that embedding the gas phase ion in the point charge array has little effect on the ion charge density. Consequently, Figure 6 shows that the eigenvalue change associated with embedding is that expected if we assume the model described by equation (2). In other words, the F^- electron density is contained within the flat portion of the

Table 3 Mulliken gross atomic basis function populations for F^-

Atomic basis functions	*Gas phase F^- ion*	*F^- ion in point charge array*	*Population of F^- orbitals in embedded $[FMg_6]^{11+}$ cluster*
*s*1	1.0415	1.0415	1.0412
*s*2	0.8890	0.8891	0.8896
*s*3	0.1831	0.1851	0.1775
*s*4	0.9752	0.9779	0.9850
*s*5	0.9093	0.9064	0.9067
*p*1	0.8112	0.8119	0.8211
*p*2	0.6864	0.6892	0.7276
*p*3	0.5022	0.4989	0.4754

Madelung potential (Figure 5). This is possible because the F^- ion is a stable gas phase species (unlike O^{2-}). The F^- ion is an example of an anion (in MgO) that is not affected by the point charge array.

3.1.4 The Mg^+ defect ion

This ion has a single unpaired 3*s* electron. In the perfect MgO lattice this electron will occupy a state in the valence band and hence have an energy above the Fermi level. In the gas phase, the outermost electron is strongly bound to the atomic centre.

Figure 7 shows that by embedding the Mg^+ ion in a point charge array, the energy level values of the gas phase ion are increased by an average of only 18.10 eV, 5.79 eV less than the Madelung energy. The applied electrostatic field has caused a significant change in the Mg^+ ion electron density. Comparison of Mulliken basis function populations for gas phase and point charge embedded ions (see Table IV), shows that the increase in orbital eigenvalues is accompanied by an expansion of the charge density away from the magnesium centre. This expansion appears as an increase in

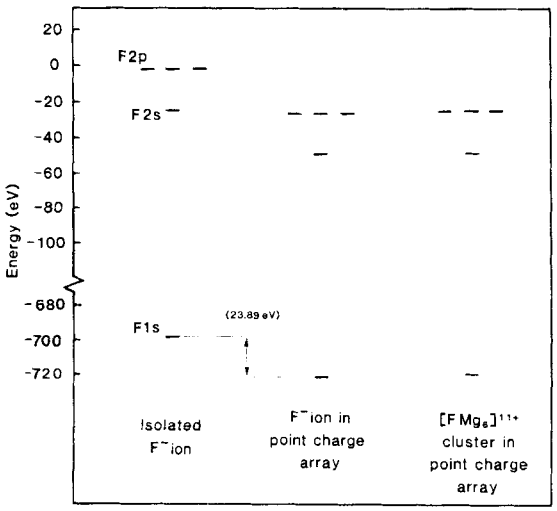

Figure 6 F^- ion energy levels calculated for the gas phase ion and for the ion embedded in two different lattice-model environments.

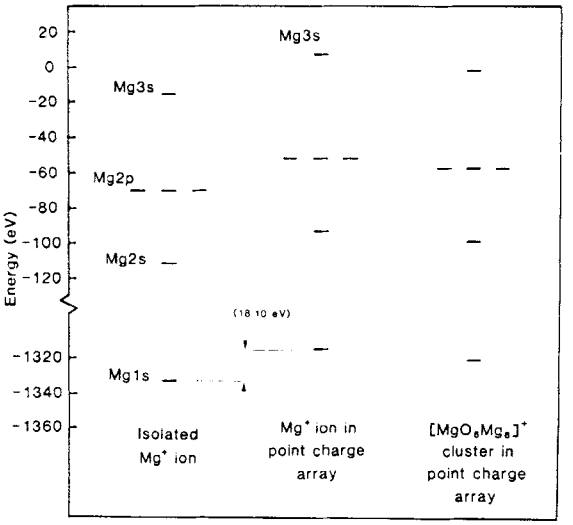

Figure 7 Mg^+ ion energy levels calculated for the gas phase ion and for the ion embedded in two different lattice-model environments.

*s*4 function population at the expense of the *s*3 function. There is little change in *p* function populations. Given this, it is reasonable to assume that the effect of the point charge array has been to delocalise the outer 3*s* electron. In fact, the Mg^+ ion undergoes this valence orbital expansion as a consequence of the interaction of the Mg^+ electron density with the Madelung potential well sides (see Figure 3). The energy of the system is lowered through delocalisation since the outer electron is then subject to a lower electrostatic potential. This effect was not observed with the Mg^{2+} ion because the energy required to extend the Mg^{2+} electron density out to the potential well sides is greater than any gain in potential energy. The Mg^+ ion is therefore an example of a cation (in MgO) which is greatly affected by an embedding environment.

3.2 The effect of nearest neighbour ions

3.2.1 The lattice O^{2-} ion

So far, the description of the lattice has included only electrostatic effects based on a

Table 4 Mulliken gross atomic basis function populations for Mg^+

Atomic basis functions	*Gas phase Mg^+ ion*	*Mg^+ ion in point charge array*	*Population of Mg orbitals in embedded $[MgO_6Mg_6]^+$ cluster*
*s*1	1.9993	1.9984	1.9984
*s*2	1.9874	1.9754	1.9866
*s*3	0.6414	−0.1272	−0.0518
*s*4	0.3719	1.1634	1.0668
*p*1	1.9596	1.9516	1.9512
*p*2	0.0456	0.0536	0.0488
*p*3	−0.0052	−0.0052	0.0000

point charge model. In real crystals, ions interact through short range electron–electron repulsion and exchange terms in addition to the long range effects that cause the Madelung potential. A more realistic lattice model can, therefore, be formed if nearest neighbour point charges are replaced by ions included within the quantum cluster. In the case of a central O^{2-} ion in MgO, this means adding six Mg^{2+} ions to form an $[OMg_6]^{10+}$ cluster (see Figure 1). Energy levels calculated for this cluster embedded in the appropriate point ion array are presented in Figure 4. This shows that the oxygen molecular orbital energies are less negative by 2.88 eV than those calculated for the single O^{2-} ion embedded in a point charge array. The increase in energy is due to further compression of the O^{2-} ion's electron density beyond that due to the point array. This is confirmed by the Mulliken population analysis of the cluster given in Table II. The population of each diffuse $p3$-type function is 0.824 for the gas phase O^{2-} ion, 0.798 for the point charge embedded ion and 0.679 for the O^{2-} ion in the embedded $[OMg_6]^{10+}$ cluster. The change in $p3$ population between the gas phase and point charge embedded ions is 0.026 electrons while the change between the point charge and embedded cluster models is 0.119. In both cases, the decrease in $p3$ population is consistent with an increase in the population of the less diffuse $p2$ function. Thus, the effect of the nearest neighbour ion electron density on the containment of the O^{2-} ions electron density is greater, although of the same order, as was the effect of the point charge array. This is in agreement with the conclusions of previous calculations [13].

The containment of the O^{2-} ions electron density by nearest neighbour Mg^{2+} ion electrons occurs because of repulsion between the electron clouds of the ions concerned. It is possible to express this repulsive interaction in terms of an orthogonalisation potential which will effectively alter the shape of the potential surface to which the O^{2-} ion is subject. This has been included schematically in Figure 5. The orthogonalisation potential will be almost zero up to a distance that corresponds to the nearest neighbour distance minus the Mg^{2+} ionic radius, that is, out to where the electron cloud of the Mg^{2+} extends. After this, the effect of the tightly bound Mg^{2+} electron density dominates and the effective potential rises. Since the potential starts at the ionic radius rather than the greater nearest neighbour distance, the orthogonalisation potential will affect ions of smaller size than the Madelung potential.

3.2.2 The lattice Mg^{2+} ion

It is difficult to use the $[MgO_6]^{10-}$ cluster to investigate the effect of nearest neighbour ions on the lattice Mg^{2+} ion. The origin of this problem is the neglect of short range forces from ions surrounding the cluster. Consequently, the very polarisable nearest neighbour O^{2-} ions of the $[MgO_6]^{10-}$ cluster polarise away from the central Mg^{2+} ion, and the eigenvalues of the Mg^{2+} molecular orbitals become less negative (see Figure 4). This is an artifact of the finite cluster model. To address the problem, it is possible to use the larger $[MgO_6Mg_6]^{2+}$ cluster (see Figure 1). This includes six additional Mg^{2+} ions (in 200 type positions) which provide some of the short range repulsive force necessary to prevent the undesirable polarisation of the O^{2-} ion. Unfortunately, because the O^{2-} ions in the $[MgO_6Mg_6]^{2+}$ cluster are not at the centre of symmetry of the cluster, there is still some polarisation of the O^{2-} ion due to unbalanced forces. This causes the small difference in eigenvalue between the Mg^{2+} ion embedded in the point charges and the central Mg^{2+} ion in the $[MgO_6Mg_6]^{2+}$ cluster. The difference is however substantially less than with the $[MgO_6]^{10-}$ cluster.

The Mulliken population for the central Mg^{2+} ion in the $[MgO_6Mg_6]^{2+}$ cluster

(Table I) shows almost no change compared with either the gas phase or point charge embedded ions. This implies that electron–electron interactions from lattice ions have little effect on the Mg^{2+} lattice ion electron density. This is consistent with results from previous investigations [13].

3.2.3 The defect F^- ion

From the results of Table III, it is apparent that at an O^{2-} vacancy site in unperturbed MgO, the electron density of the F^- ion is only slightly modified by nearest neighbour electron repulsion. Mulliken populations in Table III show a modest redistribution in charge from the $p3$ to the $p2$ basis functions. This is five times smaller than the equivalent change observed for the O^{2-} ion. In section 3.1.3, it was noted that the density is unaltered by embedding in the point charge array. These might be regarded as surprising results since the F^- ion is regarded as polarisable. However, F^- has an octahedral crystal radius of 1.33 Å [22] while the crystal radius of the O^{2-} ion (and by inference the defect site) is 1.38 Å [22]. The F^- ion is therefore easily accommodated at the oxygen vacancy site. The magnitude of the charge redistribution associated with the F^- ion will be reduced by ionic relaxations which cause the nearest neighbour ions to move radially out from the F^- ion by 0.10 Å [19].

The results for F^- do not generalize to all anion defects in MgO. For example, calculations for embedded Cl^- show significant contraction of electron density due to electron repulsion from surrounding ions [23]. This is not surprising since the Cl^- ion has a crystal ionic radius of 1.81 Å [22] which is significantly larger than even the relaxed defect site.

3.3 Lattice relaxation effects and the Mg^+ defect ion

In this study, we employ an embedded $[MgO_6Mg_6]^+$ cluster to model the effect of nearest neighbour ions on the Mg^+ electron density. The large cluster is also used to provide a physically realistic environment for the description of oxygen ion polarization (see section 3.2.2).

Introduction of cluster ions around the central Mg^+ ion decreases the Mg^+ orbital energies by 4.09 eV. This is a consequence of the polarization of the oxygen ions in response to the Mg^+ defect centre. The polarization reduces the effective electrostatic potential contribution to the central Mg^+ orbital energies. A similar but smaller effect was observed with the Mg^{2+} ion calculations in section 3.2.2. However, whereas polarisation in the $[MgO_6Mg_6]^{2+}$ cluster was entirely due to asymmetry in the short-range forces (caused by the limitation of a finite cluster model), with a central Mg^+ defect, there are physically sensible strong electrostatic forces that are responsible for polarisation in the $[MgO_6Mg_6]^+$ cluster.

By considering the population of Mg^+ basis functions in the $[MgO_6Mg_6]^+$ cluster (Table IV), it is clear that the cluster ions have acted to reduce somewhat the valence orbital expansion that resulted from embedding the gas phase ion in the point charge array. Two factors have combined to contain the Mg^+ electron density. First, the oxygen ions provide an orthogonalization potential that acts to contain the Mg^+ electron density (see Figure 3). This will also increase orbital energies (as in section 3.2.1). The second factor is specific to examples where the point charge embedded ion has a delocalised valence electron. In these cases, the nearest neighbour polarisation, in reducing the effective height of the Madelung potential, reduces the tendency for the Mg^+ outer electron to move away from the ion centre. Reducing the height of the

Madelung potential will also reduce orbital energies. Although the two factors both act to contain and localise the valence electron, they work in opposition in their effect on orbital energies. In this example, polarisation reduces orbital eigenvalues more than the orthogonalization potential raises them (see Figure 7).

The Mg^+ ion represents a somewhat extreme example. Calculations carried out on other cations do not show such extreme behaviour. In particular, for Na^+ substituted at an Mg^{2+} site, the point charge array has little effect on Mulliken basis function populations [23]. This might be expected since the crystal ion radius of Na^+ is 1.02 Å [22], much smaller than the flat portion of the Madelung well which extends out to 2.106 Å.

In the perfect MgO lattice, as defined in Figure 4, the nearest neighbour O^{2-} electron density will act to reduce the constant potential radius to about 0.72 Å. Since this is distinctly smaller than the Na^+ radius, the O^{2-} density might be expected to significantly alter the Na^+ ion electron density. However, in MgO, the Na^+ ion is a charged defect and, as such, the nearest neighbour ions relax away from the defect centre by up to 0.16 Å [19]. Given this, the size of the relaxed vacancy site is comparable with the size of the defect ion so that little change in the Na^+ electron density occurs [23].

4. CONCLUSIONS

It is clear from this work that in many cases, we expect lattice effects to be important in determining the electron density of both anions and cations embedded in a solid. Consequently, it is unrealistic to expect useful pair potentials to be derived from calculations which use the electron densities of gas phase ions. It has also been demonstrated that it is not reasonable to assume that the effect of lattice potentials is greater for anions than it is for cations. In particular, although the effect of embedding (using a lattice model environment) on the electron density of an O^{2-} ion is significant, changes to the F^- ion are minimal. Conversely, while Mg^{2+} remains unchanged, Mg^+ is greatly modified.

The last point to emphasize concerns the choice of embedding lattice model potential. It has been found that in addition to an electrostatic Madelung potential, other terms accounting for electron repulsion (between electron clouds) and exchange must be taken into account if realistic electron densities are to be calculated. In fact, in these calculations, electronic terms have been shown to be at least as important as the Madelung potential.

Acknowledgments

These calculations were carried out at the University of Keele as part of the General Nuclear Safety Research programme of the UKAEA at Harwell. The manuscript was prepared at Michigan Technological University with facilities made available in the department of Physics by Professor A. B. Kunz. The author is grateful to Susan Hill, Ravindra Pandey and Tony Harker for careful proof reading of the manuscript.

References

[1] M. Born and A. Landé, "On the calculation of the compressibility of perfect crystals from lattice theory," Verhandl. Deut. Physik Ges. Val 20, p 210, (1918), and references therein.

[2] C.R.A. Catlow, M. Dixon and W.C. Mackrodt, "Interionic potentials in ionic solids," in *Computer Simulations of Solids*, Edited by C.R.A. Catlow and W.C. Mackrodt, Springer-Verlag, Berlin, FRG, (1982).
[3] J.H. Harding, *Mol. Sim.*, **4**, 255, (1990).
[4] P.T. Wedepohl, "Influence of electron distribution on atomic interaction potentials," *Proc. Phys. Soc.*, **92**, 79, (1967).
[5] R.G. Gordon and Y.S. Kim, "Theory for the Forces between Closed-Shell Atoms and Molecules," *J. Chem. Phys.*, **56**, 3122, (1972).
[6] J.H. Harding and A.H. Harker, "The calculation of inter-atomic potentials using electron gas models," UK AERE Harwell Report R-10425, (1982).
[7] N.L. Allan, D.L. Cooper, W.C. Mackrodt, "The practical calculation of interionic potentials in solids using Electron Gas Theory," *Mol. Sim.*, **4**, 269, (1990).
[8] N.C. Pyper, "Four important factors in the *ab-initio* determination of accurate inter-ionic potentials," *Mol. Sim.*, this issue.
[9] J.H. Harding and A.H. Harker, "Calculation of interionic potentials in oxides," *Phil. Mag. B*, **51**, 119, (1985).
[10] R. Pandy and J.M. Vail, "F-type centres and hydrogen anions in MgO: Hartree-Fock ground states," *J. Phys. Condensed Matter*, **1**, 2801, (1989).
[11] J. Meng, R. Pandy, J.M. Vail and A.B. Kunz, *Phys. Rev. B*, **38**, 10083, (1988).
[12] J.Q. Broughton and P.S. Bagus, "Self-consistent-field studies of core-level shifts in ionic crystals: LiF," *Phys. Rev. B*, **30**, 4761, (1984).
[13] J.Q. Broughton and P.S. Bagus, "Self-consistent-field studies of core-level shifts in ionic crystals: II. MgO and BeO," *Phys. Rev. B*, **36**, 2813, (1987).
[14] P.W. Fowler and P.A. Madden, "In-crystal polarizabilities of alkali and halide ions," *Phys. Rev. B*, **29**, 1035, (1984).
[15] P.W. Fowler and P.A. Madden, "In-crystal polarizability of O^{2-}," *J. Phys. Chem.*, **89**, 2581, (1985).
[16] G.D. Mahan, "Polarizability of ions in crystals", *Solid State Ionics*, **1**, 29, (1980).
[17] P.W. Fowler, "A user's guide to polarizabilities and dispersion coefficients for ions in crystals," *Mol. Sim.*, **4**, 313, (1990).
[18] R.E. Watson, "Analytic Hartree-Fock solutions for O^{2-}," *Phys. Rev.*, **111**, 1108, (1958).
[19] R.W. Grimes, C.R.A. Catlow and A.M. Stoneham, "A comparison of defect energies in MgO using Mott-Littleton and quantum mechanical procedures," *J. Phys. Condensed Matter*, **1**, 7367, (1989).
[20] M.F. Guest, J. Kendrick and S.A. Pope, "Program GAMESS Documentation" SERC Daresbury Laboratory, (1983).
[21] R.S. Mulliken, "Electronic population analysis on LCAO-MO molecular wave functions," *J. Chem. Phys.*, **23**, 1833, (1955), and *J. Chem. Phys.*, p1841, p2338, and p2343.
[22] R.D. Shannon, "Revised effective ionic radii and systematic studies of interatomic distances in halides and chalcogenides," *Acta Cryst.*, **A23**, 751–767, (1976).
[23] R.W. Grimes, C.R.A. Catlow and A.M. Stoneham, unpublished details of the study in reference [19].